Journal of Mineralogical and Petrological Sciences, Volume 109, page 74–78, 2014

LETTER

Adachiite, a Si-poor member of the tourmaline supergroup from the Kiura mine, Oita Prefecture, Japan

Daisuke NISHIO-HAMANE*, Tetsuo MINAKAWA**, Jun-ichi YAMAURA*, Takashi OYAMA**, Masayuki OHNISHI*** and Norimasa SHIMOBAYASHI†

*The Institute for Solid State Physics, the University of Tokyo, Kashiwa 277-8581, Japan
**Departments of Earth Science, Faculty of Science, Ehime University, Matsuyama 790-8577, Japan
***Takehana Ougi-cho, Yamashina-ku, Kyoto 607-8082, Japan
†Department of Geology and Mineralogy, Graduate School of Science, Kyoto University, Sakyo-ku, Kyoto 606-8502, Japan

Adachiite, $CaFe_3Al_6(Si_5AlO_{18})(BO_3)_3(OH)_3(OH)$, a Si-poor member of the tourmaline supergroup, is found in the hydrothermal vein cutting emery from Nabagasako of the Kiura mine, Saiki City, Oita Prefecture, Japan. Adachiite occurs as a constituent (several to 300 μm thickness) of hexagonal prismatic crystals, and forms a zoned structure closely associated with schorl. It is transparent with brownish-purple to bluish-purple color, while the massive aggregate shows black in color. Adachiite is trigonal, $R3m$, a = 15.9290(2), c = 7.1830(1) Å, V = 1578.39(4) Å^3, and Z = 3, determined via single crystal XRD refinement (R_1 = 0.038). Adachiite is the first member of the tourmaline group formed via Tschermak-like substitution.

Keywords: Adachiite, Tourmaline supergroup, Tschermak-like substitution, New mineral, Kiura mine

INTRODUCTION

Laterite is Al-rich and Si-poor soil formed in hot and wet tropical areas, and 'emery', an ultra-hard black-colored rock consisting mainly of corundum and hercynite, is a form of lateritic metamorphic rock (Iwao, 1978). The constituent silicates in lateritic metamorphic rock are also rich in Al and poor in Si, and potassic-(ferro)-sadanagaite, one of the main constituent silicates in lateritic metamorphic rock, has the highest Al and the lowest Si content of the amphibole group. (Shimazaki et al., 1984; Nishio and Minakawa, 2003). Rare minerals such as baddeleyite, zirconolite, and calzirtite also occur within lateritic metamorphic rock (Nishio et al., 2003; Nishio and Minakawa, 2004). During mineralogical investigation of lateritic metamorphic rock involving emery, a new, Si-poor tourmaline was found in emery from the Kiura mine, Saiki City, Oita Prefecture, Japan.

This new tourmaline is named adachiite in honor of Tomio Adachi (b. 1923), a well-known amateur mineralogist who contributed to the field of mineralogy as a local guide. The mineral classification and name have been approved by the International Mineralogical Association, Commission on New Minerals, Nomenclature and Classification (no. 2012-101). The type specimen is deposited in the collections of the National Museum of Nature and Science, Tsukuba, Japan (specimen no. NSM-M43748). Here we report a new mineral, adachiite.

doi:10.2465/jmps.131020b
D. Nishio-Hamane, hamane@issp.u-tokyo.ac.jp Corresponding author

OCCURRENCE AND PHYSICAL AND OPTICAL PROPERTIES

Emery deposits were discovered in Kiura mine in 1959 and reported by Yoshimura et al. (1962). Although Yoshimura et al. (1962) used the company name 'Shin-kiura mine' the present study uses 'Kiura mine' as the more historical and popular name. Adachiite was found in a hydrothermal vein cutting the emery from Nabagasako. The hydrothermal vein consists mainly of margarite, chlorite, and diaspore, within which tourmalines, including adachiite, occur (Fig. 1). Adachiite occurs as a constituent (several to 300 μm thickness) of hexagonal prismatic crystals up to about 2 cm in length and 5 mm in

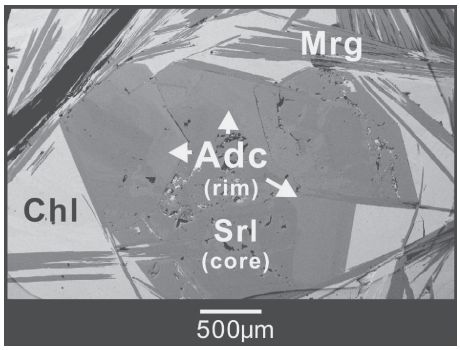

Figure 1. Back-scattered electron image for adachiite. Adc, adachiite; Chl, chlorite; Mrg, margarite; Srl, schorl.

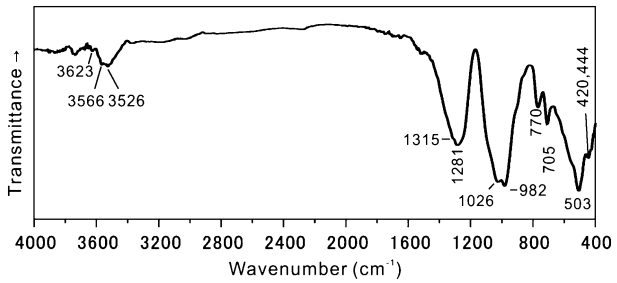

Figure 2. Fourier transform-infrared absorption (FT-IR) spectrum for adachiite.

width. It forms a zoned structure closely associated with schorl. The massive tourmaline aggregate shows black color, while small crystals (~ 1 mm) are transparent with brownish to bluish-purple color. The Mohs hardness is 7, and the calculated density is 3.228 g/cm^3. The mineral is uniaxial (-) of ω 1.674 (2) and ε 1.644 (2) (589 nm). The compatibility calculated from the refractive index and empirical formula is 0.024 (excellent). It also shows very strong pleochroism: ω, dark green to dark blue and ε, brownish-yellow.

INFRARED SPECTROMETRY

A Fourier transform-infrared absorption (FT-IR) spectrum of adachiite was recorded using a KBr pellet method on a JASCO MFT-680 FTIR spectrometer for the region 400-4000 cm^{-1} (Figure 2). Using examples from the analysis of the related material (Bačík et al., 2013), the spectrum shows the absorption bands at 400-840 cm^{-1} for the lattice vibrations, 840-1200 cm^{-1} for the $(Si,Al)_6O_{18}$ stretching vibrations and Fe-OH bending vibrations, 1200-2000 cm^{-1} for the BO_3 stretching vibrations, 3200-3600 cm^{-1} for the O-H stretching vibrations at O3, and 3600-3700 cm^{-1} for the O-H stretching vibrations at O1. The lack of absorption around 1600 cm^{-1} indicates the absence of the H_2O molecule.

Table 1. Chemical composition of adachiite

n = 13	wt%	Range	Standard		Element**
SiO_2	29.79	28.80-31.91	Quartz	Si	5.148
TiO_2	0.46	0.23-1.44	Rutil	Ti	0.060
Al_2O_3	36.70	36.19-37.45	Corundum	Al	7.475
FeO	11.90	10.84-12.06	Hematite	Fe	1.720
MgO	2.32	1.93-2.53	Periclase	Mg	0.598
CaO	3.34	2.69-3.54	Wollastonite	Ca	0.618
Na_2O	0.84	0.73-0.92	Albite	Na	0.281
B_2O_3	10.09	9.19-11.53	Takedaite	B	3.010
H_2O*	3.10				
Total	98.54				
				^{W}OH	0.561
				^{W}O	0.439

* Calculation as ^{V}OH = 3 and ^{W}O/OH ratio.
** Basis of $Y + Z + T = 15$.

CHEMICAL COMPOSITION

Chemical analyses were performed using a JEOL JXA-8105 electron microprobe (WDS mode, 15 kV, 5 nA, 3-μm beam diameter) at Kyoto University. The ZAF method was used for correction, and the results are given in Table 1. Li was not estimated because the Kiura emery deposit lacks Li-bearing minerals. F was below detectable limits (0.01 wt%). Since the tourmaline formula is shown as $XY_3Z_6(T_6O_{18})(BO_3)_3V_3W$ and the X site allows for vacancy, the empirical formula is calculated on the basis of $Y + Z + T = 15$. Fe was estimated as Fe^{2+} because of structural restraint as the ^{W}OH-type tourmaline. H_2O was calculated on the basis of an electroneutral formula as: ^{V}OH = 3 and ^{W}O/OH ratio, based on $Y + Z + T = 15$. The empirical formula on the basis of $Y + Z + T = 15$ with the crystal structure refinement is $^X(Ca_{0.62}Na_{0.28}\square_{0.10})_{\Sigma 1.00}$ $^Y(Fe_{1.58}Al_{0.81}Mg_{0.55}Ti_{0.06})_{\Sigma 3.00}$ $^Z(Al_{5.81}Fe_{0.14}Mg_{0.05})_{\Sigma 6.00}$ $^T(Si_{5.15}Al_{0.85})_{\Sigma 6.00}O_{18}B_{3.01}O_9$ $^V(OH)_3$ $^W[(OH)_{0.56}O_{0.44}]_{\Sigma 1.00}$. The ideal formula is $CaFe_3Al_6(Si_5AlO_{18})(BO_3)_3(OH)_3(OH)$, which requires SiO_2 28.09, Al_2O_3 33.37, FeO 20.15 CaO 5.24, B_2O_3 9.77, H_2O 3.37, and totals 100 wt%.

CRYSTALLOGRAPHY

Single crystal XRD data were obtained using a Bruker SMART CCD area-detector diffractometer with Mo$K\alpha$ radiation. SHELXL-97 software was employed to refine the crystal structure. The occupancies of hydrogen were fixed at 0.56 for H1 from the EPMA result, and 1.0 for H3 as the structural formula, respectively. Initial hydrogen atomic positions were estimated via difference-Fourier synthesis, and then refined on the constraint by fixing

Table 2. Data collection and details of structure refinement

Space group	$R3m$
Crystal size (mm)	0.15 × 0.06 × 0.01
a, c (Å)	15.9290(2), 7.1830(1)
V (Å^3)	1578.39(4)
Z	3
Absorption coefficient μ (mm^{-1})	2.44
No. of Reflections Measured	5589
Independent reflections	1886
R_{int}	0.040
θ_{max}(°)	40.0
Miller index limit	$-22 \le h \le 28$, $-27 \le k \le 28$ $-12 \le l \le 9$
Absorption correction method	Multiscan $T_{min} = 0.901$, $T_{max} = 0.425$
R_1 $[F^2 > 2\sigma(F^2)]$, wR_2	0.038, 0.093
S	1.09
No. of parameters	91
Restraint	Fixing O-H distaince of 0.95 Å
Weighting scheme	$w = 1/[\sigma^2(F_o^2) + (0.0285P)^2 + 8.7875P]$ Where $P = (F_o^2 + 2F_c^2)/3$
$\Delta\rho_{max}$ / $\Delta\rho_{min}$ (e Å^{-3})	1.19 / -0.80

Diffraction data were measured at 300 K using the *SAINT* program (Bruker, 2000) and an empirical absorption correction was applied using *SADABS* (Bruker, 2004). The structure was solved using Superflip (Palatinus and Chapuis, 2007).

the O-H distance. Refinement details are listed in Table 2, and the structural data are summarized in Tables 3 and 4. The structure of adachiite was refined in $R3m$ (Table 4) and converged to a final R_1 index of 3.8% (Table 2).

In the first step of the refinement, the electron numbers of sites *X*, *Y*, *Z*, and *T* were observed as a function of the occupancy of Ca, Fe, Al, and Si, respectively. The cation assignment of *Y* and *Z* sites was then adjusted using Fe and Mg contents after fixing Ti in *Y* site in accordance with the general site abundance (Henry et al., 2011) to be the minimum difference between the observed and estimated electron numbers using the EPMA result (Table 3). The cation assignment at sites *X* and *T* follows the EPMA result. As shown in the electron numbers at sites *Y* and *Z*, Al apparently occupies the *Z* site rather than the *Y* site in adachiite, and then most divalent cations are conclusively placed at the *Y* site, in good agreement with the *Y* site configurations of ^{W}OH-type tourmaline (Hawthorne and Henry, 1999; Hawthorne, 2002; Henry et al., 2011). Although direct determination of the $Fe^{3+}/\Sigma Fe$ ratio is not feasible in the present state owing to complex zoning, the $Fe^{3+}/\Sigma Fe$ ratio in adachiite might be low. If

Table 3. Cation assignments for adachiite

Site	Observed No. e-	Cation assignment from EPMA (*apfu*)	Estimated No. e-
X	15.2(2)	0.62Ca+0.28Na+0.10□ →	15.5
Y	58.0(4)	1.58Fe+0.81Al+0.55Mg +0.06Ti →	59.6
Z	77.1(5)	5.81Al+0.14Fe+0.05Mg →	79.7
T	79.9(5)	5.15Si+0.85Al →	83.1

the structure contains a significant amount of Fe^{3+}, the charge is balanced by dehydration, and then ^{W}O-type tourmaline may be derived. However, since adachiite has the structural characteristics of ^{W}OH-type tourmaline, we assume that all Fe is present as Fe^{2+} in this study. Following cation assignments, occupancies were fixed and other parameters were refined. Bosi and Lucchesi (2007) reported negative correlation <*Y*-O> and <*Z*-O> versus Al at each site for the crystal-chemical relationships in the tourmaline group. Since those of adachiite are consistent with their report (Fig. 3), the refinement for atomic distance may be reasonably converged. We also note the anisotropic thermal vibration of *Y* site, which vibrates at a slight angle relative to the *Y*-O bond plane (Table 4). This behavior is often observed in tourmaline of schorl-dravite and uvite-feruvite series such as schorl (Foit, 1989), dravite (Hawthorne et al., 1993), oxy-schorl (Bačík et al., 2013), uvite (Taylor et al., 1995), and feruvite (Grice and Robinson, 1989). *Y* polyhedra are chemically more flexible than other polyhedra, and connect by sharing O1 and O2. The anisotropic thermal behavior of *Y* site might be due to the polyhedral distortion and relatively large thermal vibration of oxygens.

The angle-dispersive X-ray diffraction (XRD) pattern was collected using a synchrotron X-ray source on the NE1 beam line of Photon Factory-Advanced Ring for Pulse X-rays (PF-AR) at the High Energy Accelerator Research Organization (KEK), Japan. This beam line provides a 30-μm diameter collimated beam of monochromatized X-ray radiation (λ = 0.4179 Å). The XRD spectrum was collected using the Debye-Scherrer method and recorded using an imaging plate detector. The XRD pattern was obtained using powder prepared from the micro sample (~ 100 μm), and is listed in Table 5.

RELATIONSHIP TO OTHER MINERALS

Tourmaline species are classified according to site occupancy and heterovalent coupled substitution such as a Tschermak-like substitution involving tetrahedral-octa-

Table 4. Final atom coordinates and displacement parameters (Å^2) for adachiite

Site	x	y	z	U_{iso}*/U_{eq}		
X	0	0	0.2081 (3)	0.0174 (3)		
Y	0.12224 (5)	0.06112 (2)	0.63623 (14)	0.00832 (11)		
Z	0.29794 (5)	0.26128 (5)	0.60922 (14)	0.00601 (12)		
T	0.19255 (5)	0.19060 (5)	0	0.00587 (11)		
B	0.10990 (13)	0.2198 (3)	0.4491 (5)	0.0070 (5)		
^{W}O1	0	0	0.7832 (9)	0.0250 (12)		
^{W}H1	0	0	0.915 (3)	0.025*		
O2	0.06050 (10)	0.12100 (19)	0.4776 (5)	0.0145 (5)		
^{V}O3	0.2673 (2)	0.13366 (11)	0.5076 (4)	0.0111 (4)		
^{V}H3	0.272 (4)	0.136 (2)	0.377 (3)	0.011*		
O4	0.09253 (11)	0.1851 (2)	0.0714 (4)	0.0142 (5)		
O5	0.1841 (2)	0.09203 (12)	0.0946 (4)	0.0140 (5)		
O6	0.19684 (13)	0.18670 (13)	0.7736 (3)	0.0087 (3)		
O7	0.28708 (12)	0.28653 (12)	0.0786 (3)	0.0083 (3)		
O8	0.20900 (13)	0.26973 (14)	0.4381 (3)	0.0089 (3)		
Site	U_{11}	U_{22}	U_{33}	U_{12}	U_{13}	U_{23}
X	0.0143 (4)	0.0143 (4)	0.0235 (9)	0.0072 (2)	0	0
Y	0.0080 (2)	0.00567 (17)	0.0121 (3)	0.00398 (12)	−0.0036 (2)	−0.00178 (10)
Z	0.0059 (3)	0.0062 (3)	0.0058 (2)	0.0030 (2)	−0.0001 (2)	0.0002 (2)
T	0.0057 (2)	0.0053 (2)	0.0065 (2)	0.00262 (19)	−0.0001 (2)	−0.00040 (19)
B	0.0072 (9)	0.0076 (12)	0.0063 (11)	0.0038 (6)	0.0002 (5)	0.0005 (10)
^{W}O1	0.0307 (19)	0.0307 (19)	0.014 (2)	0.0154 (10)	0	0
O2	0.0176 (10)	0.0044 (9)	0.0171 (12)	0.0022 (5)	0.0007 (4)	0.0014 (8)
^{V}O3	0.0189 (12)	0.0106 (7)	0.0065 (8)	0.0094 (6)	0.0011 (8)	0.0005 (4)
O4	0.0118 (7)	0.0209 (13)	0.0128 (10)	0.0104 (6)	−0.0015 (5)	−0.0031 (10)
O5	0.0206 (13)	0.0122 (7)	0.0119 (10)	0.0103 (6)	0.0001 (9)	0.0000 (5)
O6	0.0085 (7)	0.0089 (6)	0.0067 (6)	0.0028 (5)	0.0010 (5)	0.0009 (5)
O7	0.0083 (6)	0.0067 (6)	0.0079 (6)	0.0022 (5)	0.0007 (5)	−0.0001 (5)
O8	0.0063 (6)	0.0101 (7)	0.0105 (6)	0.0042 (5)	0.0000 (5)	0.0033 (5)

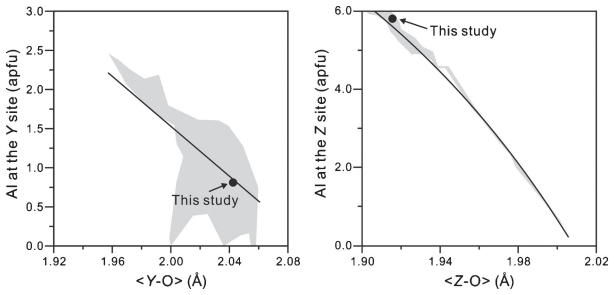

Figure 3. Bond distance versus Al plots showing the compositional dependence of the Y and Z sites. The gray area and the lines represent the range of plots and fitting curve reported by Bosi and Lucchesi (2007).

hedral site (Henry et al., 2011). Adachiite, $CaFe_3Al_6(Si_5AlO_{18})(BO_3)_3(OH)_3(OH)$, is characterized by Al in the T site, and can be compositionally formed by Tschermak-like substitution ($M^{2+} + {}^T Si^{4+} \leftrightarrow Al^{3+} + {}^T Al^{3+}$) from tourmaline in calcic-subgroup 1, $CaFe_3(MAl_5)(Si_6O_{18})(BO_3)_3(OH)_3(OH)$. Adachiite is the first tourmaline formed via Tschermak-like substitution, and conclusively has the lowest Si content. The formation of adachiite may be facilitated by the extremely high Al and low Si environment found in emery.

ACKNOWLEDGMENTS

We thank T. Nagai for assistance with the synchrotron X-ray experiment (no. 2012G050). We are grateful to S. Matsubara and the anonymous referee for their constructive reviews.

REFERENCES

Bačík, P., Cempírek, J., Uher, P., Novák, M., Ozdín, D., Filip, J., Škoda, R., Breiter, K., Klementová, M., Ďuďa, R. and Groat, L.A. (2013) Oxy-schorl, $Na(Fe^{2+}_2Al)Al_6Si_6O_{18}(BO_3)(OH)_3O$, a new mineral from Zlatá Idka, Slovak Republic and Přibyslavice, Czech Republic. American Mineralogist, 98, 485-492.

Table 5. Powder X-ray diffraction data for adachiite

h	k	l	I/I_0	$d_{obs.}$ (Å)	$d_{calc.}$ (Å)
1	0	1	23	6.3507	6.3501
0	2	1	34	4.9602	4.9745
3	0	0	27	4.6261	4.6207
2	1	1	40	4.2254	4.2249
2	2	0	65	4.0022	4.0016
0	1	2	34	3.4553	3.4589
1	3	1	17	3.3859	3.3855
2	0	2	9	3.1724	3.1750
4	0	1			3.1180
4	1	0	20	3.0241	3.0249
1	2	2	31	2.9503	2.9513
3	2	1	33	2.9027	2.9053
3	1	2			2.6168
0	5	1	100	2.5842	2.5846
0	4	2	8	2.4876	2.4872
2	4	1	11	2.4598	2.4595
0	0	3	11	2.3772	2.3812
2	3	2	11	2.3772	2.3752
5	1	1	28	2.3502	2.3510
6	0	0	8	2.3111	2.3103
1	1	3	5	2.2813	2.2824
5	2	0			2.2197
5	0	2	11	2.1918	2.1901
4	3	1	20	2.1708	2.1711
0	3	3	9	2.1160	2.1167
4	2	2	9	2.1160	2.1124
2	2	3	52	2.0428	2.0463
1	5	2	52	2.0428	2.0425
1	6	1	16	2.0264	2.0270
4	4	0	9	2.0003	2.0008
3	4	2	22	1.9204	1.9112
7	0	1	8	1.9081	1.9083
3	5	1	8	1.9081	1.9083
1	4	3	8	1.8696	1.8711
6	2	1	9	1.8565	1.8563
6	1	2	4	1.8187	1.8192
3	3	3	6	1.7764	1.7765
2	6	2	8	1.6926	1.6927
0	6	3	14	1.6586	1.6582
2	7	1	21	1.6480	1.6478
5	5	0	19	1.6011	1.6006
4	5	2	8	1.5890	1.5894
4	0	4	8	1.5890	1.5875
4	6	1	7	1.5521	1.5521
9	0	0	6	1.5401	1.5402
7	2	2	5	1.5307	1.5302
7	3	1	3	1.5233	1.5237
8	2	0	5	1.5119	1.5125
0	5	4	6	1.5014	1.5014
2	4	4	4	1.4750	1.4756
5	1	4	15	1.4523	1.4512
4	7	0	7	1.4377	1.4374
a = 16.006(2), c = 7.144(1) Å, V = 1585.1(4) Å^3					

Bosi, F. and Lucchesi, S. (2007) Crystal chemical relationships in the tourmaline group: Structural constraints on chemical variability. American Mineralogist, 92, 1054-1063.

Bruker (2000) *APEX*2, *SAINT* and *SADABS*. Bruker AXS Inc. Madison, Wisconsin, USA.

Bruker (2004) *SADABS, APEX*2, *SAINT* and *XPREP*. Bruker AXS Inc. Madison, Wisconsin, USA.

Foit, F.F. (1989) Crystal chemistry of alkali-deficient schorl and tourmaline structural relationships. American Mineralogist, 74, 422-431.

Grice, J.D. and Robinson, G.W. (1989) Feruvite, a new member of the tourmaline group, and its crystal structure. The Canadian Mineralogist, 27, 199-203.

Hawthorne, F.C. (2002) Bond-valence constraints on the chemical composition of tourmaline. The Canadian Mineralogist, 40, 789-797.

Hawthorne, F.C., MacDonald, D.J. and Burns, P.C. (1993) Reassignment of cation occupancies in tourmaline: Al-Mg disorder in the crystal structure of dravite. American Mineraogist, 78, 265-270.

Hawthorne, F.C. and Henry, D.J. (1999) Classification of the minerals of the tourmaline group. European Journal of Mineralogy, 11, 201-215.

Henry, D.J., Novák, M., Hawthorne, F.C., Ertl, A., Dutrow, B.L., Uher, P. and Pezzotta, F. (2011) Nomenclature of the tourmaline-supergroup minerals. American Mineralogist, 96, 895-913.

Iwao, S. (1978) Re-interpretation of the chloritoid-, staurolite- and emery-like rocks in Japan - chemical composition, occurrence and genesis. Journal of the Geological Society of Japan, 84, 49-67.

Nishio, D. and Minakawa, T. (2003) The titanian esseneitic diopside in Al-skarn from Myojin and Mutsuki islands in Seto Inland Sea, Japan. Japanese Magazine of Mineralogical and Ptrological Sciences, 32, 68-79 (in Japanese with English abstract).

Nishio, D., Minakawa, T. and Noto, T. (2003) Emery from Ko-Oge Island in Ryoke Terrane, Seto Inland Sea, Japan. Japanese Magazine of Mineralogical and Ptrological Sciences, 32, 159-167 (in Japanese with English abstract).

Nishio, D. and Minakawa, T. (2004) Baddeleyite, zirconolite and calzirtite in lateritic rocks from Ryoke and Chichibu Terranes, Japan. Journal of Mineralogical and Petrological Sciences, 99, 42-53.

Palatinus, L. and Chapuis, G. (2007) Superflip - a computer program for the solution of crystal structures by charge flipping in arbitrary dimensions. Journal of Applied Crystallography, 40, 786-790.

Shimazaki, H., Bunno, M. and Ozawa, T. (1984) Sadanagaite and magnesio-sadanagaite, new silica-poor members of calcic amphibole from Japan. American Mineralogist, 69, 465-471.

Taylor, M.C., Cooper, M.A. and Hawthorne, F.C. (1995) Local charge-compensation in hydroxyl-deficient uvite. The Canadian Mineralogist, 33, 1215-1221.

Yoshimura, T., Furukawa, H. and Aoki, Y. (1962) Emery deposits recently found at the Shin-Kiura mine, Oita Prefecture, Japan. Mining Geology, 56, 346-352 (in Japanese with English abstract).

Manuscript received October 20, 2013
Manuscript accepted January 16, 2014
Published online April 5, 2014
Manuscript handled by Kazumasa Sugiyama